Digital Twin Simulation of a Battery Energy Storage System for On-Grid Applications

Singh Sathya Prakash*, Yu Zhenyong, Li Chengqiang, Ke Fei, Dong Zili, and Zhao Shaozhong

R&D Department, ZheJiang HuaBang IOT Technology Co., Ltd, Wenzhou, Zhejiang, 325103, China
Email: 15258043575@163.com (S.S.P.)
*Corresponding author
Manuscript received October 28, 2024; accepted May 7, 2025; published August 18, 2025.

***Abstract*—Digital twin technology is transforming the management and optimisation of Battery Energy Storage Systems (BESS) in on-grid applications. This paper presents the design and simulation of a digital twin for BESS with the aim of identifying system performance, reliability and operational efficiency through mathematical modelling. A detailed simulation-based architecture is developed, enabling predictive analytics and control. The digital twin uses a Single Particle Model (SPM) to computationally simulate the electrochemical behaviour of battery cells, providing insight into critical parameters such as State of Charge (SoC), State of Health (SoH) and degradation over time. In addition, a Python-based simulation model is examined to analyse and optimise energy flows within the grid. This study demonstrates how simulation-driven digital twin technology can enhance decision-making and system control in on-grid BESS applications, making it useful for academic studies and practical implementation.**

***Keywords*—digital twin, battery energy storage system, on-grid application, single particle model, python, SoC, SoH, predictive maintenance, energy management system**

I. Introduction

The urgent need to reduce carbon emissions and achieve net-zero targets has spurred a global transition towards sustainable energy, necessitating a shift to renewable sources like solar and wind. The rapid growth of renewable energy, particularly wind and solar, has increased their share in electricity from 21% to 29%, with global capacity reaching 3,372 GW by the end of 2022 [1]. Projections indicate that renewables will account for 42% of global electricity generation by 2028, with solar and wind expected to contribute 96% of new capacity additions [2]. However, their intermittency poses challenges for grid stability, highlighting the need for innovative solutions.

One such solution is Battery-Based Energy Storage Systems (BESS) which can be critical for a cleaner, resilient power infrastructure, smoothing out fluctuations from renewable sources and enhancing grid stability [3]. Key battery types include lithium-ion, lead-acid, sodium-sulfur, and emerging solutions such as solid-state batteries [4]. Battery technologies are projected to evolve significantly by 2030, focusing on the circular economy with a capacity of 4.7 TWh and a cost of $80/kWh [5]. The performance parameters—energy density, power density, cycle life, efficiency, and safety—determine their suitability for various applications. Integrating BESS into the electricity grid presents technical, economic, regulatory, and market challenges [6]. Growing demand, driven by supportive policies and technological advancements, is making BESS more cost-competitive, despite challenges like high initial costs and safety concerns. BESS applications extend across transportation, industry, and residential sectors, providing mobile energy storage in electric vehicles and energy independence in homes. Energy Management Systems (EMS) and Battery Management Systems (BMS) are essential for optimizing BESS performance. Together, they enhance grid stability and flexibility, supported by AI and predictive analytics. To further enhance the capabilities of Battery Energy Storage Systems (BESS), the integration of Digital Twin technology emerges as a transformative approach that promises to elevate system performance, monitoring, and control to unprecedented levels [7]. Digital twins refer to a digital representation of physical systems that can provide real-time data synchronization, allowing for monitoring, analysis, and optimization. Digital Twins facilitate the creation of a virtual testing environment, enabling the simulation of various operational scenarios for BESS prior to actual implementation. This innovative technology allows for comprehensive evaluation and optimization of system behavior under diverse conditions, thereby enhancing decision-making and improving overall operational effectiveness.

II. Literature Review

The integration of diverse modeling approaches within Battery Energy Storage Systems (BESS) establishes a robust foundation for the accurate prediction and optimization of battery performance, health, and longevity [8]. Central to this system is the Battery Management System (BMS), which facilitates real-time monitoring by assessing critical metrics such as State of Charge (SOC) and State of Health (SOH), while concurrently identifying faults [6]. Emerging capabilities within BMS seek to incorporate predictive analytics, thus enabling projections of Remaining Useful Life (RUL) and facilitating early anomaly detection to support proactive maintenance strategies. Control system models further enhance operational efficiency by dynamically managing charge-discharge cycles, thermal regulation, and grid integration, thereby ensuring optimal BESS performance under varying load conditions [9]. The reliability of BESS is underpinned by advanced electrical models. Equivalent circuit models, such as RC and Thevenin, offer simplified analyses of battery behavior and facilitate SOH estimation through internal resistance tracking; however, they are limited in their capacity to capture detailed aging patterns. In contrast, electrochemical models [10] provide a granular examination of battery reactions, monitoring the development of the Solid Electrolyte Interphase (SEI) layer and associated chemical reactions, which improves the

DOI: 10.7763/IJET.2025.V17.1322

accuracy of SOH and RUL estimations. Hybrid models that integrate data-driven methodologies with electrochemical approaches leverage machine learning techniques to enhance predictions of both RUL and fault risks [11]. Thermal and safety models [12] play a crucial role in managing the thermal dynamics of batteries, addressing heat generation and dissipation to mitigate thermal stress, thereby promoting battery longevity. Additionally, these safety models focus on potential hazards, including thermal runaway, and incorporate data derived from thermal assessments to ensure the safety of BESS applications, particularly in critical contexts. Degradation modeling [13] addresses both chemical and physical alterations over time; specifically, electrochemical aging models track the growth of the SEI layer and lithium depletion, which gradually diminish capacity and augment impedance. Multi-physics models converge electrochemical, thermal, and mechanical factors to comprehensively monitor degradation, while stochastic models simulate real-world variability in temperature and load, refining predictive accuracy under fluctuating operational scenarios.

In the grid interactions, DC-AC power electronics models assess the impact of power conversion on BESS efficiency, which is vital for grid-connected systems. Furthermore, lifecycle cost analysis models quantify total ownership costs and returns, thereby facilitating sustainable financial planning for large-scale BESS projects [14]. Lastly, grid interaction models enhance the functionality of BESS within the dynamics of the grid and demand-response applications, enabling functionalities such as peak shaving and frequency regulation, which bolster coordination between distributed energy resources and the grid [14].

As the field of battery technology evolved, the emphasis shifted toward applications requiring real-time data and optimization capabilities. The emergence of digital twin technology represents a crucial advancement in this context. Digital twins serve as virtual representations of physical systems that utilize real-time data to enable dynamic simulations and performance forecasting. This functionality renders digital twins indispensable for the proactive management of battery systems within broader energy frameworks, including power grids [15].

The convergence of advanced modeling techniques and digital twin technology signals the dawn of a new era in energy storage and grid management. These advancements are poised not only to enhance the management and integration of battery technologies but also to propel the development of intelligent, adaptive, and sustainable energy systems. This integrative approach addresses the complexities inherent in battery aging, thermal effects, and safety considerations, ensuring that BESS deployments remain economically viable, safe, and technically proficient in real-world environments [16].

This paper examines the integration of Digital Twin Simulation on-grid Battery Energy Storage Systems (BESS), focusing on developing an architecture that enhances operational efficiency, energy management, and grid support functions. Through the Single Particle Model (SPM) as a foundation for battery modeling, this study explores methods to simulate, monitor, and optimize BESS performance. Python programming is employed to bring theoretical models into practical application, enabling data-driven insights that inform battery behavior, and predictive maintenance. This approach not only contributes to a more responsive BESS architecture but also demonstrates the digital twin's potential in optimizing energy storage solutions within on-grid systems. Although this paper covers only limited part of the above section due to lack of data availability.

III. Materials and Methods

The digital twin framework for on-grid Battery Energy Storage Systems (BESS) offers a comprehensive representation that integrates the Communication Layer, Digital Twin Layer, and Analytics and Control Layer, facilitating a seamless digital replica of the physical system [17]. This framework encompasses a wide array of components, including hardware, software, and communication protocols, ensuring that real-time performance metrics such as State Of Charge (SOC), State Of Health (SOH), voltage, temperature, and Remaining Useful Life (RUL) are accurately captured and modeled.

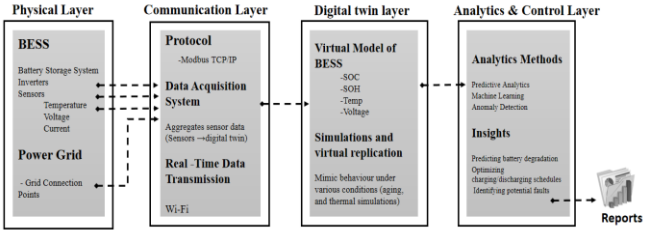

Fig. 1. Overview of the system architecture for digital twin integration on-grid systems.

Considering a battery packs, with an average capacity of 210 kWh and a cycle life of 3500 cycles, are central core to the system. Sensors, such as temperature, Voltage sensors, Aerosol to capture critical data. Power converters and inverters facilitate the conversion of DC power to AC power. Circuit breakers, fuses and pre-charge circuits to ensure system protection. Grid connection points, adhering to standards like IEEE 1547, enable grid integration.

The Communication and Data Layer enables data exchange through robust protocols and networks, transmitting real-time sensor data to cloud storage for further analysis. The Digital Twin Model leverages this data, simulating system dynamics and providing actionable insights for optimizing operations and performing predictive maintenance (18). Integration with the grid enables peak shaving, load leveling, and enhances grid resiliency, while machine learning algorithms drive predictive analytics to anticipate system failures, ensuring the longevity and efficiency of the BESS. Finally, cloud platforms handle large-scale data processing, with visualization tools offering intuitive dashboards that empower stakeholders to make informed decisions and optimize system performance.

The evolution of battery models, especially in the context of digital twin technology, has shifted from simplistic empirical approaches to advanced physics-based modeling techniques. This shift underscores the necessity for a deeper understanding of the complex interactions governing battery performance.

Considering the $LiFePO_4$ - graphite system, the electro-chemical storage reactions in charge can be represented by

Eqs. (1) & (2) as:

Positive electrode:

$$Li_yFePO_4 \xrightarrow{Charge} yLi^+ + ye^- + Li_{1-y}FePO_4 \quad (1)$$

Negative electrode:

$$xLi^+ + xe^- + Li_{1-x}C_6 \xrightarrow{Charge} Li_xC_6 \quad (2)$$

The controlled voltage source for conventional batteries can be expressed in a mathematical model [19] as:

$$V = V_0 - K \cdot \frac{Q}{Q - \int idt} - R_{elec} i + Ae^{-B\int idt} \quad (3)$$

where V: battery voltage (V), V_0: no-load battery voltage (V), K: polarization voltage (V), Q: battery capacity (Ah), R_{elec}: internal resistance (Ω), i: battery current (A), A: exponential zone amplitude (V), B: inverse of the charge at the end of the exponential zone $(Ah)^{-1}$.

The Eq. (3) and associated models were computationally efficient, they lacked the capability to accurately capture the intricate electrochemical reaction, thermal effects, and kinetics transport phenomena within lithium-ion battery and behavior. This limitation motivated the transition to more sophisticated physics-based models.

The Pseudo-Two-Dimensional (P2D) model [20] emerged as a significant advancement, integrating electrochemical reactions, mass transport, and thermal dynamics. Despite its comprehensive nature, the high computational cost of the P2D model restricted its real-time applicability in Battery Management Systems (BMS). In response to these limitations, there has been a drive to develop simplified frameworks that retain essential characteristics and insights while reducing computational complexity.

The Single Particle Model (SPM) [21] addressed some these challenges by simplifying the battery representation. It assumes uniform lithium-ion concentration in the electrolyte and models lithium diffusion in a single spherical particle using Fick's law:

$$\frac{\partial C_S}{\partial t} = D_S \Delta^2 C_S \quad (4)$$

where: C_s is the lithium concentration in the solid phase (mol/m^3), D_s is the solid-state diffusion coefficient (m^2/s).

Boundary conditions for lithium diffusion are:

At the particle surface

$$-Ds\frac{\partial Cs}{\partial r}\bigg|_{r=R} = \frac{I}{a_S F} \quad (5)$$

flux is proportional to the current density.

At the particle center (r=0)

$$\frac{\partial Cs}{\partial r} = 0 \quad (6)$$

ensures symmetry

The SPM's simplicity allows for faster simulations with lower computational demands, making it suitable for certain applications. However, it neglects electrolyte dynamics and becomes less accurate under high charge/discharge rates, where ionic transport resistance and concentration polarization effects are significant. To overcome the limitations, the Single Particle Model with Electrolyte (SPMe) incorporates the effects of electrolyte concentration and potential are critical for accurate modeling [22, 23]. This extension uses concentrated solution theory to model ionic transport resistance, electrolyte depletion, and high C-rate operations. By bridging the gap between the simplicity of SPM and the comprehensiveness of the P2D model, SPMe improves accuracy while maintaining computational efficiency.

The distribution of lithium ions in the electrolyte is governed by the diffusion equation coupled with ionic flux [11]:

$$\frac{\partial C_e}{\partial t} = (D_e \Delta^2 C_e) - \frac{1 - t^+}{F} \Delta \cdot j \quad (7)$$

where: C_e is the electrolyte concentration (mol/m^3), D_e is the electrolyte diffusion coefficient (m^2/s), t^+ is the transference number (dimensionless), j is the ionic flux (A/m^2), F, Faraday Constant (96487 C/mol).

The electrolyte concentration directly impacts the availability of lithium ions for intercalation into the electrode material [24], the depletion or uneven distribution of C_e can lead to localized concentration polarization, reducing battery efficiency and lifetime.

The potential within the electrolyte is determined by ionic conductivity and the flux of ions [24]:

$$\Delta\varphi_e = -\frac{\Delta \cdot j}{\sigma_e} - \frac{2RT}{F}\left(1 - t^+\right)\Delta \ln C_e \quad (8)$$

where: σ_e is the electrolyte conductivity (S/m) and ϕ_e is the electrolyte potential (V).

Variations in ϕ_e affect the electrochemical potential of reactions and, subsequently, the voltage profile of the battery during operation. Modeling ϕ_e provides insights into limitations imposed by electrolyte transport resistance, enabling optimization of material properties and cell design.

The interaction between the electrolyte and solid phase is governed by interfacial reaction kinetics as shown in the Fig. 2, as described by the Butler-Volmer Eq. [25]:

$$j = j_0\left[\exp\left(\frac{\alpha_a F\eta}{RT}\right) - \exp\left(\frac{\alpha_c F\eta}{RT}\right)\right] \quad (9)$$

where j: Reaction Current density (A/m^2), j_0: Exchange current density (A/m^2), α_a, α_c Anodic and cathodic charge transfer coefficients, R: Ideal Gas constant, T: Temperature (K), η: overpotential (V).

The coupling of electrolyte dynamics with solid-phase diffusion allows accurate prediction of concentration gradients, voltage drop, and limitations under high C-rate conditions. Accurate modeling of electrolyte dynamics allows for the prediction of these gradients and helps to prevent issues like concentration polarization, which can hinder performance.

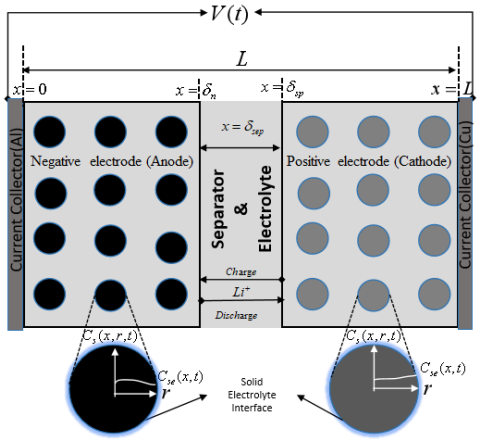

Fig. 2. Schematic of unit cell model coupled with microscopic (*r*-direction) solid -Liquid diffusion model [26].

The Average Model (AM) is predicated on fixed electrolyte concentration assumptions and charge estimation [27]. Whereas the extended AM incorporates both electrochemical and thermal dynamics, thereby enhancing its predictive capacity regarding voltage behavior and capacity recovery for battery materials across a range of charge-discharge scenarios. The cell voltage V(t) [8] is a fundamental parameter in lithium-ion battery modeling, serving as a critical link between electrochemical processes, transport phenomena, and external performance.

$$V(t) = U_p\left(\frac{C_{s,surf,p}}{C_{s,max,p}}\right) - U_n\left(\frac{C_{s,surf,n}}{C_{s,max,n}}\right) - \frac{R_{SEI,p}I(t)}{\varepsilon_{s,p}\delta_p A} - \frac{R_{SEI,n}I(t)}{\varepsilon_{s,n}\delta_n A} + \frac{RT}{\alpha F}\ln\left(\frac{\frac{-R_{s,p}}{6\varepsilon_{s,p}i_{0,p}A\delta_p}I(t) + \sqrt{\left(\frac{R_{s,p}}{6\varepsilon_{s,p}i_{0,p}A\delta_p}I(t)\right)^2 + 1}}{\frac{R_{s,n}}{6\varepsilon_{s,n}i_{0,n}A\delta_n}I(t) + \sqrt{\left(\frac{R_{s,n}}{6\varepsilon_{s,n}i_{0,n}A\delta_n}I(t)\right)^2 + 1}}\right) + (1-t_+)\frac{2RT}{F}\ln\frac{c_e(L,t)}{c_e(0,t)} - \frac{I(t)}{2A}\left(\frac{\delta_n}{k_n^{eff}} + 2\frac{\delta_{sep}}{k_{sep}^{eff}} + \frac{\delta_p}{k_p^{eff}}\right) \quad (10)$$

where U_p, U_n: Open Circuit Potential at Positive Electrode and Negative Electrode

$C_{s,max,n}$, $C_{s,max,p}$ Maximum Li-Ion Inventory at negative & positive electrode surface (mol/m^3)

$C_{s,surf,p}$, $C_{s,surf,n}$ Lithium-Ion concentration at solid electrolyte interface positive & negative (mol/m^3)

$k_n^{eff}, k_{sep}^{eff}, k_p^{eff}$ Effective Ionic Conductivity of electrolyte at different region (negative, separator and positive electrodes) of the cell (S/m)

t_+: Li^+ Transference number

F: Faraday constant (C mol^{-1})

$C_e(L), C_e(0)$: Average electrolyte Concentration (mol/m^3)

α: Charge transfer Coefficient

$R_{s,p}$, $R_{s,n}$: Radius of the positive and negative electrode spherical particles

I: Applied Current.

$\varepsilon_{s,p}$, $\varepsilon_{s,n}$ Active material Positive & Negative Volume fraction (%)

$i_{0,p}$, $i_{0,n}$ Exchange current density (A/m^2)

A: surface area of the current collector (m^2)

δ_n δ_p δ_{sep} δ_{sei} negative electrode, positive electrode, Separator and SEI layer thickness (m)

The above Eq. (10), represents the dynamic interplay of Open-Circuit Voltage (OCV), Impact by SEI growth, electrochemical reaction kinetics described by the Butler-Volmer equation, and internal resistive effects, making it an essential input for accurately simulating battery behavior. V(t) provides a comprehensive framework to understand key aspects such as State Of Charge (SOC), power capability, thermal impacts and quantifying the impact of the variations of design parameters during aging. The parameter values used in Eqs. (10) and (11) are directly adopted from the work of He *et al.* (22).

The OCP of an LFP cell is determined by the electrochemical potential of the lithium ions present in the cathode and anode materials [28]. For cathode material $LiFePO_4$ Eq. (11) stoichiometry varies with respect to "x_{sp}"

$$U_P = 3.432 - 0.8428e^{-80.249(1-x_{sp})^{1.319}} - 3.247\times10^{-6}e^{20.264(1-x_{sp})^{3.8}} + 3.2482\times10^{-6}e^{20.264(1-x_{sp})^{3.799}} \quad (11)$$

The functional form of the negative OCV curve fitted equation for anode/graphite

$$U_n = 0.638 + 0.542e^{-305.5309x_{sn}} + 0.044\tanh\left(-\frac{x_{sn}-0.196}{0.109}\right) - 0.198\tanh\left(\frac{x_{sn}-1.057}{0.085}\right) - 0.686\tanh\left(\frac{x_{sn}+0.012}{0.053}\right) - 0.018\tanh\left(\frac{x_{sn}-0.569}{0.086}\right) \quad (12)$$

Solid Electrolyte Interphase (SEI) layer [29], the Impact by SEI growth:

$$-\frac{R_{SEI,p}I(t)}{\varepsilon_{s,p}\delta_p A};-\frac{R_{SEI,n}I(t)}{\varepsilon_{s,n}\delta_n A} \quad (13)$$

The SEI layer resistance is

$$R_{SEI,j} = \frac{L_{SEI}}{k_{SEI}} \quad (14)$$

where K_{SEI} is the SEI layer conductivity and SEI layer thickness L_{SEI}

The SEI layer thickness is

$$k_{SEI} = k_{SEI0}e^{\frac{-E_{a2}}{RT}} \quad (15)$$

where E_{a2} is the activation energy for SEI layer thickness growth, and k_{SEI0} is the SEI layer growth coefficient.

SEI layer thickness

$$L_{SEI} = \frac{0.1Q_{in}M_{SEI}}{A_j n_{SEI}\rho_{SEI}F} \quad (16)$$

where the Q_{in} is the battery capacity before the SEI layer formation cycle process is conducted (100%), A_n, A_p is the particle surface area before the SEI layer formation cycle, n_{SEI} is the number of lithium moles lost for every mole of SEI

layer formed, ρ_{SEI} is the SEI layer density, and M_{SEI} is the molecular weight of compounds constituting the SEI layer.

The initial surface area of the single particle is the surface area of a sphere with initial defects.
where

$$A_n = 4\pi R_{s,n}(1+2\rho_{cr}l_{cr0}a_0),\ A_p = 4\pi R_{s,p}(1+2\rho_{cr}l_{cr0}a_0) \quad (17)$$

where l_{cro} is the initial defect width, a_0 is the initial defect length, $R_{s,n}, R_{s,p}$ is the particle radius, and ρ_{cr} is the number of cracks per unit area.

Ohmic resistance, Eq. (10),

$$R_{ohm} = \frac{1}{2A_{n,p}}\left(\frac{\delta_n}{k_n^{eff}} + 2\frac{\delta_{sep}}{k_{sep}^{eff}} + \frac{\delta_p}{k_p^{eff}}\right)$$

$$k_j^{eff} = k_j\varepsilon_{e,j}^{Brugg,n} = k_j(1-\varepsilon_{f,j}-\varepsilon_{s,j})^{Brugg,j} \quad (18)$$

$$k_{sep}^{eff} = k_j\varepsilon_{e,sep}^{Brugg,sep} = k_j(1-\varepsilon_{s,sep})^{Brugg,sep} \quad (19)$$

where ε_e and ε_f ε_e and ε_f of the electrolyte and filler, and from the Bruggman exponent, *Brugg*, of each region.

The dynamic nature of surface stoichiometry not only governs electrochemical reaction rates but also reflects the immediate availability of lithium ions for intercalation or deintercalation. The surface lithium concentration at the electrode-electrolyte interface at the positive and negative electrode gives:

Positive Electrode:

$$SOC_{Cell} = 100\times\left(\frac{x_{s,j}-x_{s,j,0\%}}{x_{s,j,100\%}-x_{s,j,0\%}}\right) \quad (20)$$

where:

$x_{s,j}$ and $x_{s,j}$ represents the current stoichiometry at the surface of the negative & positive electrode.

$x_{s,j,0\%}$ and $x_{s,j,0\%}$ is the negative and positive electrode stoichiometry at 0% SOC.

$x_{s,j,100\%}$ and $x_{s,j,100\%}$ is the negative and positive electrode stoichiometry at 100% SOC.

IV. Result and Discussion

The research aims to provide insights and practical methodologies for advancing BESS integration in contemporary grids, by addressing key operational challenges, and promoting efficient energy dispatch and utilization. This study employs a Digital Twin (DT) framework to simulate a 210 kWh Battery Energy Storage System (BESS), incorporating detailed cell-level parameters and operational data, validating its effectiveness as a simulation tool for grid integration. The Single Particle Model with Electrolyte (SPMe) incorporates the effects of electrolyte concentration and potential are critical for accurate modeling, dynamic interplay of Open-Circuit Voltage (OCV), Impact by SEI growth, electrochemical reaction kinetics described by the Butler-Volmer equation, and internal resistive effects-based SOC estimation proved resilient against sensor noise and load fluctuations, maintaining consistency with physical measurements under dynamic operating conditions.

The voltage V(t) as a function of time can be expressed utilizing its governing equations, providing insights into the dynamic response of the battery during operation. During rapid charge and discharge cycles, significant concentration gradients can develop between the surface and the bulk of the electrode, with the surface often exhibiting distinct lithium concentrations. The surface layer, where most electrochemical reactions occur, is exceptionally thin—typically ranging from a few nanometers to micrometers—and constitutes a small fraction of the electrode's total volume. Despite its limited volume, the surface plays a significant role in battery performance.

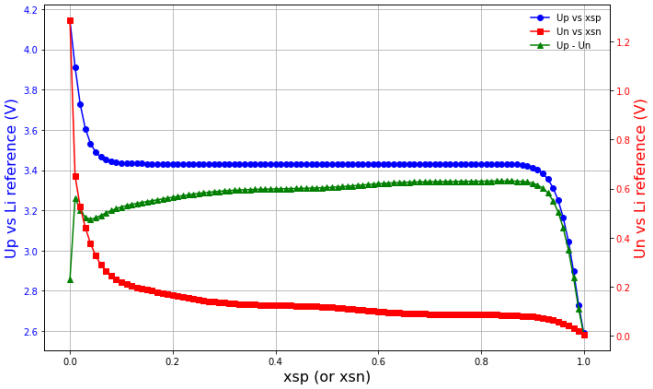

Fig. 3. Open circuit voltage of the full cell, OCV

Here dynamic hysteresis is observed, as the diffusion phenomena in the solid particles have already been considered. The thermodynamic equilibrium potentials of each electrode in charge and discharge, and based on the experimentally determined stoichiometries xsp defined in Eqs 11 and 12. The open circuit voltage of the full cell, OCV, can be reconstructed for both charge and discharge, as represented in Fig. 3. The mean of the charge and discharge OCV data is the input to a nonlinear least square procedure to perform the estimation of the electrode composition ranges.

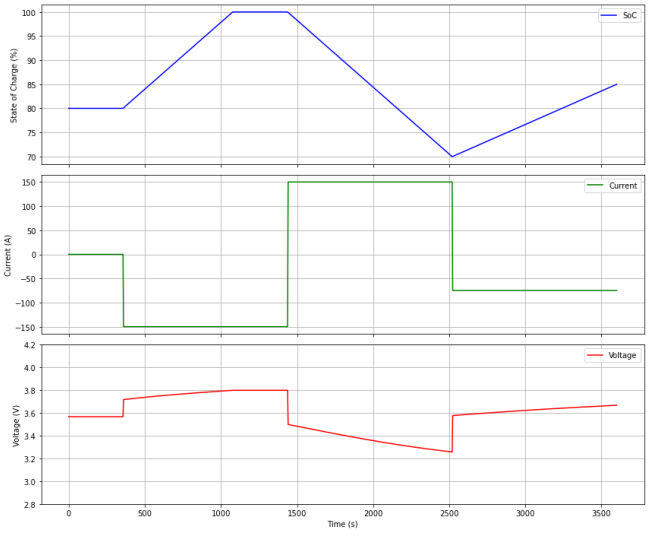

Fig. 4. Simulation results of an LFP battery using an improved voltage model showing 4a (top) State of Charge (SoC), 4b (middle) applied current profile, and 4c (bottom) terminal voltage response over time during charge and discharge cycles.

The second Fig. 4a shows SoC evolution over one hour, fluctuating between 79–80%, reflecting real-time responsiveness to transient currents and internal diffusion,

ideal for grid services like frequency regulation. The Fig 4b plot simulates applied current, alternating between charging and discharging windows, mimicking real-world energy dispatch scenarios such as peak shaving and load balancing. This current profile correlates with the SoC, aiding condition-based maintenance strategies neglecting thermal behavior.

The Fig. 4c plot shows terminal voltage, linked to SoC, providing feedback for inverter control and BMS logic, useful for safety protocols and anomaly detection. Close alignment between these curves demonstrates the model's reliability for real-world grid operations, ensuring precise energy dispatch and load balancing. These plots collectively illustrate how real-time State of Charge (SoC) measurements from the BESS, when compared with simulated outputs from the Single Particle Model (SPM), enhance the accuracy of the digital twin framework.

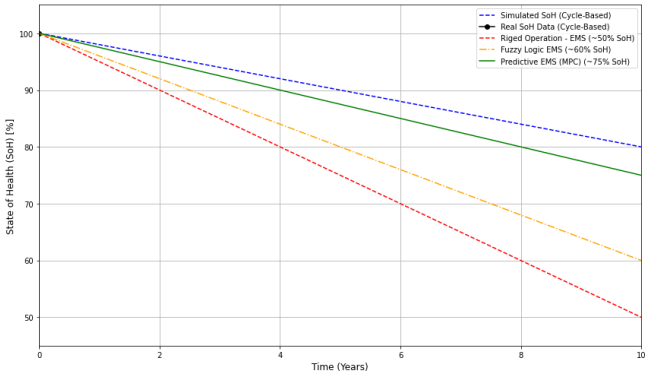

Fig. 5. Comparison of SoH degradation over 10 years under different EMS strategies: Rule-Based, Fuzzy Logic, and Predictive (MPC), against simulated and real cycle-based SoH data. Predictive EMS shows superior longevity with ~75% SoH retention

As shown in Fig. 5. the blue dashed curve represents a simulated State-Of-Health (SoH) trajectory for an LFP battery, declining linearly from 100% to 80% over 3,500 full equivalent cycles (mapped onto a 10-year timeline), consistent with empirical degradation expectations where SEI growth, lithium plating, and mechanical stress cause ~20% capacity fade after ~3,000–4,000 cycles. The graph compares this cycle-based aging with EMS-driven degradation, revealing how control strategies critically impact longevity. Considering rigid operation logic based EMS [30] (red dashed) shows the steepest decline (~65% SoH at 10 years), while fuzzy logic (31) (orange dash-dot) improves retention (~70% SoH) through dynamic rule-based optimization. Predictive EMS (MPC, green solid) outperforms both, preserving ~75% SoH by leveraging a digital twin for real-time optimization of charge/discharge actions via load forecasting and internal state modeling. Early-life empirical data (black dots) validates slower degradation than simulation, emphasizing that advanced EMS strategies—particularly MPC-minimize cumulative stress to extend operational life. This degradation analysis, vital for BESS lifecycle modeling, demonstrates the digital twin's predictive capabilities.

Fig. 6. demonstrates the alignment between significant SoH drops and actual failure points (marked in red), validating the digital twin's capability for early fault detection. Such insights enable EMS-driven preemptive control actions to mitigate cascading failures.

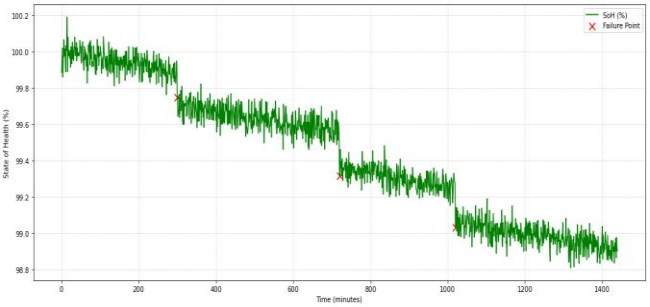

Fig. 6. SoH degradation and failure correlation over time.

Early detection of risks—such as thermal runaway or capacity plunge—enables grid-scale interventions, enhancing system reliability, fault tolerance, and compliance with safety regulations critical to utility-scale deployment.

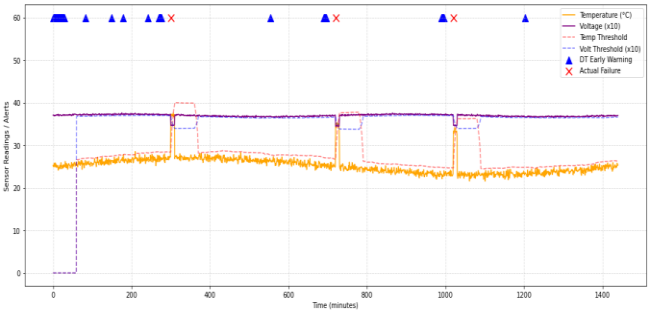

Fig. 7. Digital twin-based early warning system using MPC-style adaptive thresholds for temperature and voltage. Blue triangles indicate predictive alerts, while red crosses mark actual failures.

Fig. 7. presents a multi-parameter monitoring framework for detecting early signs of failure in a battery system using a digital twin approach. The parameters include temperature (°C), scaled voltage (×10), static safety thresholds (dashed lines), and adaptive warning thresholds derived from a Model Predictive Control (MPC)-style strategy. The orange and purple curves represent the raw temperature and voltage data respectively, showing fluctuations across multiple charge/discharge cycles. Static safety thresholds (red and blue dashed lines) serve as baseline failure limits, while the adaptive thresholds (light purple and orange markers) dynamically evolve based on system behavior, capturing transient anomalies. Blue triangles mark instances where the digital twin predicted early warnings, while red crosses indicate actual failure events. Notably, the early warnings occur well in advance of failures, validating the effectiveness of the adaptive thresholding mechanism. This adaptive digital twin approach enables proactive load scheduling and thermal management by forecasting potential failure modes. By integrating such real-time feedback into the EMS decision loop, the system can dynamically optimize power dispatch, reduce battery stress, and extend overall system life. This coupling of predictive health monitoring with EMS functionality improves resilience and asset utilization in grid-connected and off-grid applications.

The Fig. 8 illustrates the dynamic impact of a BESS digital twin on grid energy flow (in kW) across a 24-hour cycle. The blue line shows the baseline grid power flow without digital twin optimization, while the red dashed line represents the grid flow after real-time adjustments made by the digital twin.

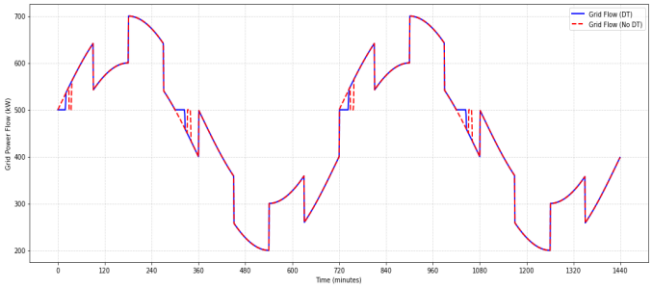

Fig. 8. Grid Energy Flow (kW) comparison with and without Digital Twin EMS.

The observed deviations, particularly during load ramps and valleys, highlights the Digital Twin's effectiveness in peak shaving, valley filling, and mitigating power fluctuations. The plot contrasts baseline (unoptimized) energy distribution with DT-controlled scenarios, highlighting reductions in peak demand, smoother ramping, and improved renewable integration. This level of control helps reduce grid stress, defer infrastructure upgrades, and enhance demand response strategies. By simulating battery behavior in real time and predicting load trends, the digital twin enables more intelligent and adaptive dispatch of BESS assets, aligning with economic and technical grid objectives.

V. Conclusion

The digital twin leverages a Single Particle Model (SPM) to simulate the electrochemical behavior of battery cells, enabling early-stage insights into key parameters like State Of Charge (SoC), State Of Health (SoH), and degradation trends. A Python-based simulation model complements this by analyzing and optimizing energy flows within the grid. Through comparative EMS analysis of various control strategies, the results show that predictive, intelligent energy management can significantly extend battery life and operational efficiency. However, the paper has a limited scope and is based on assumptions and computational limitations, which fall short of the objective. The digital twin also serves as an early warning system, identifying potential faults before they escalate, while supporting maintenance scheduling, dispatch optimization, and lifecycle planning—all within SoH-safe operating limits. Ultimately, this approach not only enhances reliability and grid stability but also paves the way for scalable, cost-effective adoption of battery energy storage systems in large-scale renewable-integrated power networks.

Appendix

This study did not generate new unique reagents. This paper does not report original code. Data reported in this paper will be shared by the corresponding author upon request. The test data was taken from a testing facility.

Conflict of Interest

The authors declare no conflict of interest.

Author Contributions

Sathya Prakash Singh worked on conceptualization (unified BESS framework), methodology (technical-financial KPI integration), project administration; Yu Zhenyong worked on software (Python dashboard development), data curation (SOC tracking, load-pattern analytics); Li Chengqiang worked on modeling (degradation analysis), formal analysis (energy-density trade-off optimization); Ke Fei workred on methodology (financial metrics: LCOS/NPV/IRR), validation (scenario simulations); Dong Zili worked on investigation (empirical validation: 1MW/2MWh LFP-BESS case study); Zhao Shaozhong wrote original draft, visualization (engineering-commercial insights); all authors had approved the final version.

References

[1] IRENA (2020). Abu Dhabi. [Online]. Available: /-/media/Files/IRENA/Agency/Publication/2020/Apr/IRENA_Global_Renewables_Outlook_2020.pdf

[2] IRENA. Abu Dhabi. International Renewable Energy Agency (IRENA). Renewable Capacity Statistics 2021. IRENA, 2021

[3] Y. C. Chang, H. C. Chang, and C. Y. Huang, "Design and implementation of the battery energy storage system in DC micro-grid systems," *Energies*. 2018, http://dx.doi.org/10.3390/en11061566

[4] G. L. Soloveichik, "Battery technologies for large-scale stationary energy storage," *Annu Rev Chem Biomol Eng.*, 2010, http://dx.doi.org/10.1146/annurev-chembioeng-061010-114116

[5] A. Jäger-Waldau, *Snapshot of Photovoltaics—February 2020*, Energies, vol. 13, 2020.

[6] Z. Y. Yu, H. W. Zhang, S. S. Prakash, Y. Y. Lyu, X. P. Wu, and D. Z.. "Review of battery energy storage systems: Challenges, strategies and applications," *Int. J. Eng. Technol.*, vol. 17, no. 1, pp. 81–89, 2025.

[7] C. Semeraro, H. Aljaghoub, M. A. Abdelkareem, A. H. Alami, and A. G. Olabi, "Digital twin in battery energy storage systems: Trends and gaps detection through association rule mining," *Energy*, 2023, http://dx.doi.org/10.1016/j.energy.2023.127086

[8] E. Prada, D. D. Domenico, Y. Creff, J. Bernard, V. Sauvant-Moynot, and F. Huet, "Simplified electrochemical and thermal model of LiFePO4-Graphite Li-Ion batteries for fast charge applications," *J. Electrochem. Soc.*, vol. 159, no. 9, 2012, https://dx.doi.org/10.1149/2.064209jes

[9] H. W. Zhang, Z. Y. Yu, S. P. Singh, Y. Y. Lyu, Z. L. Dong, and S. Z. Zhao, "Review of battery energy storage systems: Advancements and applications in power systems," *J. Electr. Power Energy Syst.*, vol. 8, no. 2, pp. 44–56, 2024.

[10] K. Liu, Y. Gao, C. Zhu, K. Li, M. Fei, C. Peng *et al.*, "Electrochemical modeling and parameterization towards control-oriented management of lithium-ion batteries," *Control Eng. Pract.*, vol. 124, 2022. https://www.sciencedirect.com/science/article/pii/S0967066122000715

[11] S. Singh, Y. E. Ebongue, S. Rezaei, and K. P. Birke, "Hybrid modeling of lithium-ion battery: Physics-informed neural network for battery state estimation," *Batteries*, vol. 9, 2023.

[12] Y. Gao, C. Zhu, X. Zhang, and B. Guo, "Implementation and evaluation of a practical electrochemical- thermal model of lithium-ion batteries for EV battery management system," *Energy*, vol. 221, 2021. https://www.sciencedirect.com/science/article/pii/S036054422032795X

[13] A. Carnovale and X. Li, "A modeling and experimental study of capacity fade for lithium-ion batteries," *Energy AI*, vol. 2, 2020, https://www.sciencedirect.com/science/article/pii/S266654682030032X

[14] D. Zhang, X. Cai, C. Song, J. Liu, J. Ding, C. Zhong *et al.,* "Life-cycle economic evaluation of batteries for electeochemical energy storage systems," *J. Electr. Eng. Technol.*, 2021, http://dx.doi.org/10.1007/s42835-021-00808-3

[15] W. Li, D. Cai, S. Wu, G. Zhang, and F. Zhang, "A multi-purpose battery energy storage system using digital twin technology," *Int. J. Electr. Power Energy Syst.*, 2024, http://dx.doi.org/10.1016/j.ijepes.2024.109881

[16] P. Mancarella, N. Hatziargyriou, and C. Kang, "Guest editorial: Special section on battery energy storage systems for net-zero power systems and markets," *J. Mod. Power Syst. Clean Energy*, 2024, http://dx.doi.org/10.35833/mpce.2024.000243

[17] Z. Jiang, H. Lv, Y. Li, and Y. Guo, "A novel application architecture of digital twin in smart grid," *J. Ambient Intell. Humaniz Comput.*, vol. 13, no. 8, pp. 3819–35, 2022. https://doi.org/10.1007/s12652-021-03329-z

[18] V. K. Saini, A. Seervi, R. Kumar, A. Sujil, M. A. Mahmud, and A. S. Al-Sumaiti, "Cloud energy storage based embedded battery technology

architecture for residential users cost minimization," *IEEE Access*, 2022, http://dx.doi.org/10.1109/access.2022.3168599

[19] O. Tremblay, L. A. Dessaint, and A. I. Dekkiche, "A generic battery model for the dynamic simulation of hybrid electric vehicles," in *Proc. 2007 IEEE Vehicle Power and Propulsion Conference*, 2007, pp. 284–289.

[20] D. Dessantis, P. D. Prima, D. Versaci, J. Amici, C. Francia, S. Bodoardo *et al.*, "Aging of a lithium-metal/LFP cell: Predictive model and experimental validation," vol. 9, *Batteries*, 2023.

[21] J. Li, N. Lotfi, R. G. Landers, and J. Park, "A single particle model for lithium-ion batteries with electrolyte and stress-enhanced diffusion physics," *J. Electrochem. Soc*., vol. 164, no. 4, 2017. https://dx.doi.org/10.1149/2.1541704jes

[22] W. He, T. Han, H. Song, Q. Wang, J. Kang, J. V. Wang *et al.*, "An extended single-particle model of lithium-ion batteries based on simplified solid-liquid diffusion process," *iScience*, vol. 27, no. 11, 2024. https://doi.org/10.1016/j.isci.2024.110764

[23] P. Kemper and D. Kum, "Extended single particle model of Li-Ion batteries towards high current applications," in *Proc. 2013 IEEE Vehicle Power and Propulsion Conference (VPPC)*, 2013, pp. 1–6.

[24] E. Olugbade and J. Park, "Boosting predictive accuracy of single particle models for lithium-ion batteries using machine learning," *Appl. Phys. Lett*., vol. 125, no. 14, 2024. https://doi.org/10.1063/5.0230376

[25] L. Liang, L. Liang, and L. Q. Chen, "Nonlinear phase field model for electrodeposition in electrochemical systems," *Appl. Phys. Lett*., vol. 105, 2014, https://www.semanticscholar.org/paper/57c4d5938538170773c155773b455a919688a663

[26] M. Guo, G. Sikha, and R. E. White, "Single-particle model for a lithium-ion cell: Thermal behavior," *J. Electrochem Soc*., vol. 158, no. 2, 2011, https://dx.doi.org/10.1149/1.3521314

[27] J. Wang, J. Meng, Q. Peng, T. Liu, X. Zeng, G. Chen *et al.*, "Lithium-ion battery state-of-charge estimation using electrochemical model with sensitive parameters adjustment," *Batteries*, vol. 9, 2023.

[28] M. Safari and C. Delacourt, "Modeling of a commercial graphite/LiFePO4 cell," *J. Electrochem Soc*., vol. 158, no. 5, 2011, https://dx.doi.org/10.1149/1.3567007

[29] F. B. Planella and W. D. Widanage, "A single particle model with electrolyte and side reactions for degradation of lithium-ion batteries," *Appl Math Model*, vol. 121, pp. 586–610, 2023. https://www.sciencedirect.com/science/article/pii/S0307904X22005959

[30] K. El Harouri, S. El Hani, N. Naseri, E. Elbouchikhi, M. Benbouzid, and S. Skander-Mustapha, "Hybrid control and energy management of a residential system integrating vehicle-to-home technology," *Designs*, vol. 7, 2023.

[31] O. Ibrahim, M. J. A. Aziz, R. Ayop, A. T. Dahiru, W. Y. Low, M. H. Sulaiman *et al.*, "Fuzzy logic-based particle swarm optimization for integrated energy management system considering battery storage degradation," *Results Eng.*, vol. 24, 2024. https://www.sciencedirect.com/science/article/pii/S2590123024010715